Available online at www.eccomasproceedia.org
Eccomas Proceedia COMPDYN (2025) 5429-5442

ECCOMAS
Proceedia

COMPDYN 2025
10th ECCOMAS Thematic Conference on
Computational Methods in Structural Dynamics and Earthquake Engineering
M. Papadrakakis, M. Fragiadakis (eds.)
Rhodes Island, Greece, 15-18 June 2025

SELECTION OF SEISMIC MODELLING APPROACH FOR CANADIAN REINFORCED CONCRETE SHEAR WALL BUILDINGS BASED ON THEIR SEISMIC BEHAVIOUR CHARACTERIZATION

D. Rodriguez[1], **F. Fazileh**[1], **and R. Fathi-Fazl**[1]

[1] Construction Research Centre, National Research Council Canada
1200 Montreal Road, Ottawa, Ontario, K1A 0R6
e-mail: derek.rodriguez@nrc-cnrc.gc.ca, farrokh.fazileh@nrc-cnrc.gc.ca, gholam-reza.fathi-fazl@nrc-cnrc.gc.ca

Abstract

To conduct the performance assessment of seismic force modification factors (SFMFs) for seismic force-resisting systems (SFRS) in National Building Code of Canada (NBC), the characterization of their seismic behaviour is a crucial step. The behaviour characterization is usually conducted by defining several archetypes representing different configurations that together are capable of describing the overall range of permissible design configurations of the SFRS. For reinforced concrete shear wall wall buildings in Canada, the modelling approach of the archetype needs to be carefully selected depending on the archetype configuration and dynamic characteristics. This ensures that it is capable of simulating the main seismic response mechanism of the reinforced concrete shear walls. At the same time, the computational efficiency of the selected modelling approach also becomes crucial, given that the calibration of SFMFs usually requires the execution of a significant number of non-linear time history analyses depending on the number of identified archetypes. There are several parameters that influence the seismic response of reinforced concrete shear walls. Among the most influential parameters are the shear span-to-depth ratio, the axial load, the detailing, the ductility level, and the cross section of the shear walls. This paper summarizes ongoing efforts at the National Research Council Canada to establish a systematic approach to select the modelling approach for different archetypes of Canadian reinforced concrete shear wall buildings based on the different configurations and dynamic characteristics to quantify their SFMFs. For this purpose, several available computationally efficient modelling approaches are identified that are suitable to simulate the seismic response of reinforced concrete shear walls with different geometric, and loading characteristics. A case study example is presented for the validation and comparison of the selected modelling approaches using reverse cyclic test data of a reinforced concrete shear wall.

Keywords: reinforced concrete, shear walls, modelling approach, seismic behaviour characterization, computational efficiency

Peer-review under responsibility of the organizing committee of COMPDYN 2025.
doi: 10.7712/120125.1282 .25077

1 INTRODUCTION

Since the birth of the practical earthquake-resistant design of structures in the beginning of the twentieth century [1], its design philosophy has been constantly evolving as new research is conducted, and new lessons are learned from the occurrence of earthquakes around the world. Nowadays, most of the seismic design provisions specified by modern codes are based on simplified force-based procedures, which make use of seismic force modification factors (SFMFs) to account for the non-linear response of the seismic force-resisting system (SFRS) when utilizing elastic analysis results to conduct the seismic design. When it comes to the Canadian context, the National Building Code of Canada (NBC) [2] introduced in the 2005 edition the two SFMFs that are currently used to conduct the seismic design of Canadian SFRSs: 1) the ductility-related factor (R_d), and 2) the overstrength-related factor (R_o).

Ideally, SFMFs should be calibrated to meet specific performance objectives, given that these factors link the seismic design process with the expected performance of the SFRS. In the United States, the FEMA P695 [3] establishes a standardized and scientifically-based methodology for the quantification of SFMFs (referred to as "seismic performance factors") for SFRSs for their inclusion in seismic design provisions. More recently, Fazileh et al. [4] proposed a performance-based unified (PBU) procedure for the quantification of SFMFs in Canada. The PBU procedure is based on the FEMA P695 methodology and further modified to allow for the consideration of several performance objectives, given that the FEMA P695 only considers a collapse prevention performance objective for the quantification of the SFMFs. Furthermore, the PBU procedure is devised to optimize the number of archetypes through a two-level screening procedure using a non-linear pushover and non-linear time history analyses (NLTHAs) in order to minimize the need for running incremental dynamic analysis (IDA). This feature allows the PBU procedure to reduce the computational overhead required to quantify SFMFs for a given SFRS.

In spite of the availability of different methodologies for the proper quantification of SFMFs, most of modern code provisions, including the NBC, specify SFMFs that are solely based on engineering judgment and/or qualitative comparisons of seismic response characteristic of different SFRSs. As a result, the actual performance of most SFRSs designed using these SFMFs is uncertain at best.

At present, the National Research Council Canada is conducting efforts towards quantifying SFMFs for reinforced concrete (RC) shear wall buildings using the PBU procedure. One of the first steps to quantify SFMFs, is to conduct the behavior characterization of the SFRS by establishing a representative sample of building archetypes that are capable of describing the overall range of permissible design configurations of the system. In the case of RC shear wall buildings, the behaviour characterization process is specially challenging due to the variety of response mechanisms that RC shear walls exhibit, and the associated difficulties to simulating these response mechanisms through numerical modelling. This paper presents a systematic procedure for selecting the numerical modelling approach of RC shear wall buildings designed according to the NBC and the CSA A23.3 [5] with the objective of quantifying their corresponding SFMFs. For this purpose, a set of numerical modelling approaches with varying computational efficiency and accuracy are identified to simulate the seismic response of RC shear walls with different geometric and dynamic characteristics. A simple comparison between two of the adopted numerical modelling approaches is presented using the experimental reverse cyclic response of a RC shear wall to illustrate the rationale behind the implemented procedure.

2 OVERVIEW OF THE PROPOSED APPROACH

Figure 1 shows a flowchart illustrating the systematic procedure proposed to select the numerical modelling approach for RC shear wall buildings designed according to the NBC and CSA A23.3.

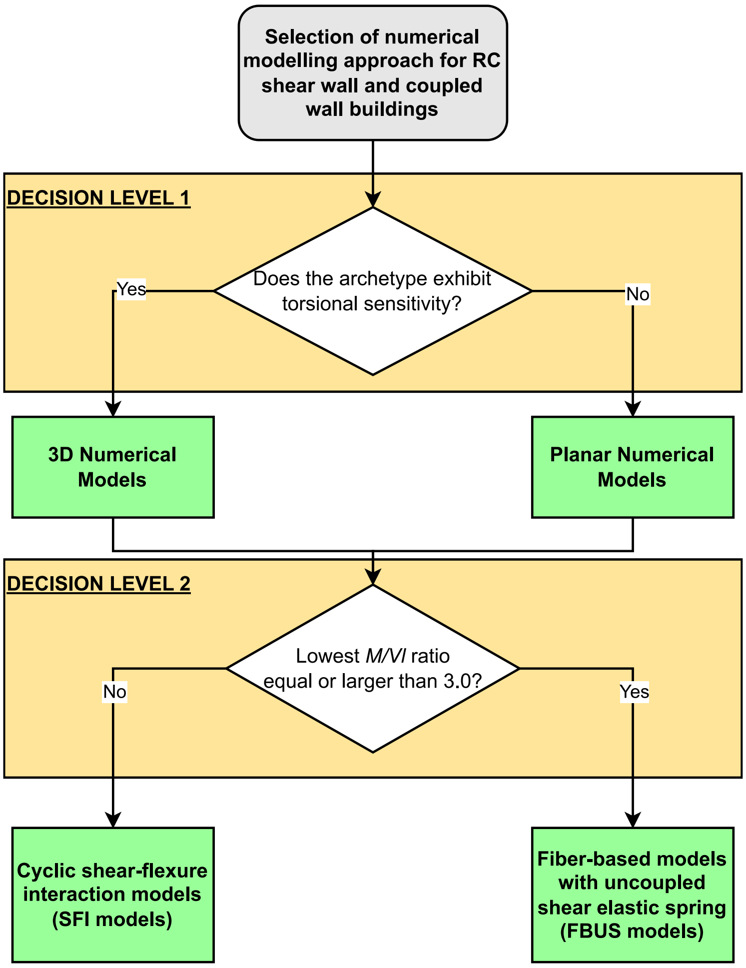

Figure 1. Definition of the numerical modelling approach for shear wall buildings designed according to the NBC and the CSA A23.3

As shown in Figure 1, the proposed procedure consists of two decision levels. In the first decision level (Decision Level 1), it must be determined if the building archetype has torsional sensitivity irregularity. According to the NBC, a building can be considered to exhibit torsional sensitivity if the ratio B exceeds 1.7. The ratio B is defined as the maximum of all values of B_x in both orthogonal directions. The ratio B_x for each building level is defined as follows:

$$B_x = \delta_{max}/\delta_{ave} \tag{1}$$

where:

δ_{max}= Maximum storey displacement at the extreme points of the structure at the level x in the direction of the earthquake induced by the forces determined according to Sentence 4.1.8.11(7) of the NBC acting at distances $\pm 0.10 D_{nx}$ from the centres of mass at each floor.

δ_{ave}= Average of the displacements at the extreme points of the structure at level x produced by the forces determined in Sentence 4.1.8.11(7) of the NBC.

D_{nx}= Plan dimension of the building at level x perpendicular to the direction of seismic loading being considered.

Buildings with torsional sensitivity can exhibit an uneven force and moment distribution within the elements of the SFRS. This behaviour arises mainly from a significant eccentricity between the centre of stiffness and the centre of mass of a particular level of the SFRS. This can produce an increase in the vulnerability of the building under seismic loading, and significantly influence the performance of the SFRS. Because of this, in the proposed procedure 3D numerical models are recommended for buildings exhibiting torsional sensitivity. By explicitly modelling the plan and elevation distribution of the elements that are part of the SFRS, the corresponding seismic force and moment distributions resulting from the eccentric building layout can be accurately evaluated. On the other hand, if the RC shear wall building archetype does not exhibit torsional sensitivity, simplified planar numerical models are recommended for the performance assessment process.

The second decision level (Decision Level 2) of the procedure consists of determining the expected seismic response mechanism of the RC shear walls. When it comes to the flexural and shear deformation contributions to the overall response and failure mode, RC shear walls are usually characterized in terms of their shear span-to-depth ratio (M/Vl). Slender elements with M/Vl ratios larger than 2.5-3.0 usually exhibit flexure-controlled response, while squat elements with M/Vl ratios less than 1.0-1.5 typically show shear-controlled responses. Shear walls with M/Vl ratios between 1.0-3.0 can exhibit responses that can be significantly influenced by both flexural and shear deformations. It is worth mentioning that in the NBC, the shear span-to-depth ratio is defined slightly differently. In the NBC, this ratio is defined as h_w/l_w, where h_w is the height of the shear wall above the section of maximum moment, and l_w is the horizontal length of the wall. Figure 2 illustrates the determination of the M/Vl ratio for a laterally loaded shear wall.

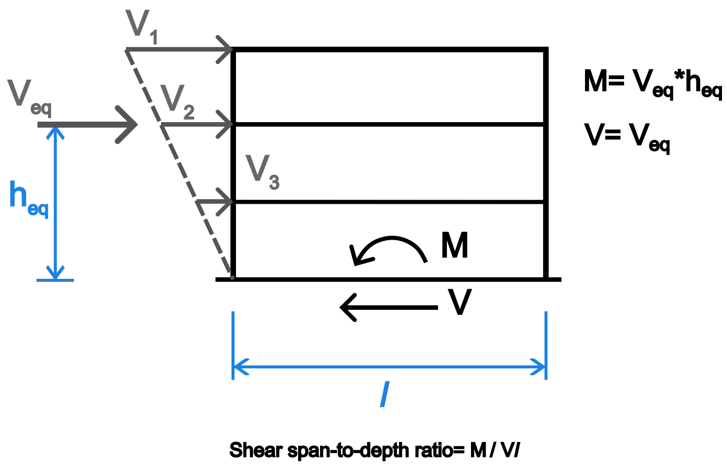

Figure 2. Illustration of the determination of the shear-span-to-depth (M/Vl) ratio of a laterally loaded shear wall.

In the case of shear walls that have flexure-controlled responses, their response can be accurately simulated with the use of fiber-based models, which account explicitly for the axial-flexural interaction at the cross section through stress-strain relationships for concrete and reinforcing steel. In this type of model, the shear behavior is not accounted for explicitly, but can be included by using a horizontal spring in the model element with a pre-defined shear-force vs deformation relationship (FBUS models). However, one of the drawbacks of this modelling approach is that the shear and axial-flexural responses are uncoupled, and therefore no interaction between them is considered in the model. As a result, this modelling approach is usually unfit to accurately simulate the response of shear-controlled elements, given that it tends to overestimate the lateral load capacity of the shear wall [6].

To deal with this limitation of fiber models, some authors have proposed shear-flexure interaction models (SFI models), which capture the interaction between axial-flexural and shear behaviour of RC shear walls [7]. While these models allow for a more rigorous simulation of the seismic response of RC shear walls, they come at the cost of longer computational times, and are sometimes more prone to experiencing convergence issues. Since the quantification of SFMFs typically requires a significant computational overhead due to the number of NLTHAs that need to be conducted, the use of such models should be limited to the cases in which they are strictly necessary, given that their widespread use within the RC shear wall building archetype database could make the analysis process unfeasible. In the proposed procedure, it is recommended to implement SFI models in cases in which the lowest M/Vl ratio of the RC shear walls within the archetype is lower than 3.0. In case in which the M/Vl ratio is equal or larger than 3.0, FBUS models are recommended.

Another type of model that has been implemented in the past to simulate the response of RC shear walls, is the lumped plasticity model [8,9]. However, such models have a series of shortcomings for the simulation of the seismic response of RC shear walls. Firstly, they are not capable of accounting for the migration of the neutral axis along the shear wall cross section during loading and unloading. Secondly, the influence of the variation in axial load on the wall strength and stiffness is not explicitly considered. Finally, the implementation of lumped plasticity models to simulate the response of non-planar walls can be challenging, which would make their use in 3D numerical models especially difficult. Considering the latest improvements in computational capabilities, in the authors' opinion, there is not a strong reason to prioritize lumped plasticity models over FBUS models for simulating the seismic response of RC shear wall buildings. Therefore, this type of model is not being considered in the proposed procedure.

It is worth mentioning that the proposed procedure could also be applicable to coupled wall buildings. In such cases, the main difference with respect to shear wall buildings is that then non-linear response of the coupling beams must be explicitly accounted for. In this type of SFRS, significant energy dissipation takes place in the coupling beams as a consequence of their shear hysteretic response. Depending on the geometry of the coupling beams, their hysteretic response can be simulated by means of non-linear shear springs located at the midpoint of elastic beams elements. These non-linear shear springs can be calibrated according to reverse-cyclic experimental data of RC coupling beams, such as those reported by Galano & Vignoli [10], and Naish et al. [11].

Finally, the numerical modelling of a given archetype is finalized by including the additional elements that are required to model the floor systems and the gravity load-resisting system (GLRS). For 3D numerical models, the floor systems and the GLRS can be explicitly modelled using elastic elements in combination with non-linear hinges. On the other hand, for planar numerical models, depending on the characteristics of the archetype, the floor systems can be modelled through rigid diaphragm elements, and the GLRS though a leaning column to account for the P-Delta effect produced by the gravitational loads in the building.

The numerical modelling approaches proposed in this systematic procedure have the advantage of combining computationally efficiency in cases that the shear walls in the building archetypes are expected to have flexure-controlled responses, and more comprehensive (but less computationally efficient) models in cases that the archetypes responses are expected to be significantly influenced by shear deformations. At the same time, it allows for saving computational overhead in cases where the RC shear wall building archetypes do not present torsional sensitivity, and can therefore be modelled by using planar models with reasonable accuracy.

Two key aspects to be evaluated when implementing this procedure, are the required computational time and accuracy of the two approaches adopted to model the response mechanisms of RC shear walls. More specifically, the SFI and FBUS models present a series of advantages and disadvantages for modelling the dynamic response of RC shear walls that were briefly discussed in this section. In the following section, a simple comparison of these models is presented to appraise their computational efficiency and accuracy in predicting the reverse cyclic response of a moderate M/Vl ratio wall, and the corresponding fragility curves calculated by means of IDA. The conducted comparison illustrates the benefits and limitations of these two modelling approaches, and the rationale behind their adoption for the proposed procedure.

3 COMPARISON OF SFI MODEL VS FBUS MODELS

In this section, the reverse cyclic response of one of the RC shear wall specimens tested by Tran and Wallace [12] was used to compare the computational efficiency and accuracy of SFI and FBUS models. The specimen RW-A15-P10-S78 tested under reverse cyclic loading was selected to conduct the comparison. This specimen had a height equal to 1829 mm, a width equal to 1219 mm, and a thickness equal to 152 mm. The specimen was laterally loaded at the top using a displacement-based reverse cyclic loading protocol. Its M/Vl ratio was approximately equal to 1.5; therefore, its response is likely to be significantly influenced by both axial-flexural and shear deformations. More details of the tested specimen can be obtained from Tran and Wallace [12].

To conduct the numerical modelling of the RC shear wall specimen, the open-source platform OpenSees [13] was used. All plots were generated using the open-source Python library Matplotlib [14]. To build the SFI model, the material and element models proposed by Kolozvari et al. [7] were used. For the selected RC shear wall specimen, the same authors provide a calibration of the SFI model in Kolozvari et al. [15] and Kolozvari et al. [16], which was used to recreate the numerical response of the specimen.

Regarding the FBUS model, the calibration of the numerical model was conducted using the "Concrete02" and the "Steel02" material models from the OpenSees material library to simulate the response of concrete and reinforcement steel fibers, respectively. Confined concrete properties were considered to model the boundary elements of the RC shear wall, while unconfined concrete properties were assumed for the web of the RC shear wall. The peak tensile stress, peak compressive stress, and corresponding strain for both the confined and unconfined concrete were taken equal to the ones of the calibrated SFI model. The yield stress, and the strain hardening ratio of the reinforcement steel were also considered equal to the ones of the calibrated SFI model. The fiber section of the RC shear wall was discretized following the recommendations provided by Pugh [17]. Several iterations were conducted to optimize the assumed number of fibers along the local axes of the cross section.

As it was mentioned in Section 2, fiber models are not capable of considering explicitly the contribution of shear deformations to the overall response of the RC shear wall. To account for the influence of shear deformations in the response of the RC shear wall specimen, a horizontal elastic spring was specified and aggregated to the fiber section using the "section aggregator" function in OpenSees. This function adds a force-deformation relationship to the pre-defined fiber section; however, this aggregation only superposes the axial-flexural and shear responses, so no interaction is considered at the section or element level. Finally, a "forceBeamColumn" element using the aggregated section with seven integration points was implemented to finalize the numerical model.

Two different values of the shear stiffness were considered in the FBUS model to appraise its influence in the obtained hysteretic response: i) a shear stiffness equal to $0.5GA_g$, and ii) a shear stiffness equal to $0.1Gk_sA_g$ as recommended by Pugh [17], where k_s is taken equal to $5/6$ for planar walls. It was found that the second option yielded closer approximations to the experimental response; therefore, it was the one considered to conduct the comparison against the SFI model.

The comparison between the numerical modelling approaches was firstly conducted based on the hysteretic response of the RC shear wall, and the absorbed energy (E_{abs}) time history. The absorbed energy was defined as the integration over time of the base shear experienced by the RC shear wall integrated with respect to its displacement. The hysteretic response in terms of base shear vs top displacement, and the absorbed energy time history for the two modelling approaches are shown in Figure 3 and Figure 4, respectively. In the same figures, the simulated hysteretic responses and absorbed energy time histories are compared against the ones obtained using the experimental test data.

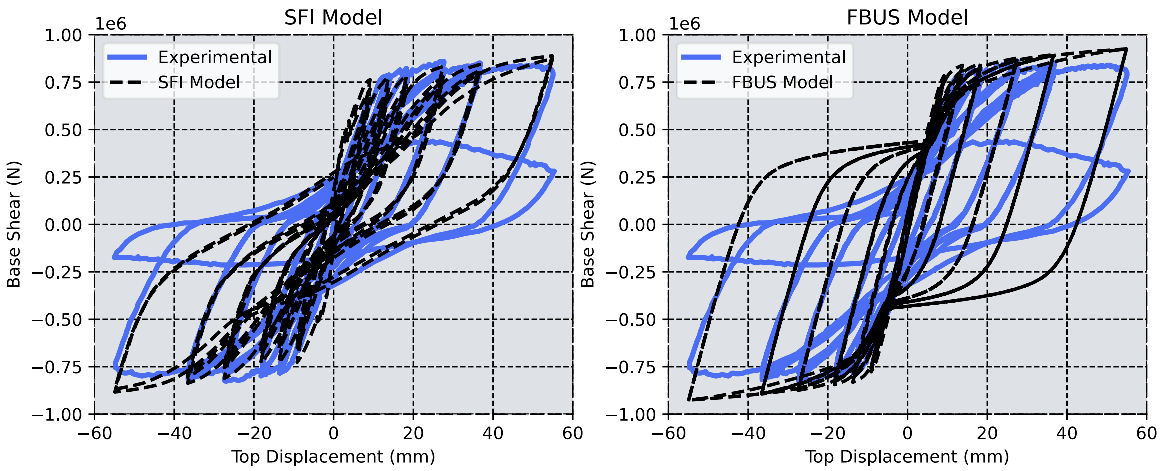

Figure 3. Comparison of the hysteretic response in terms of base shear against top displacement predicted by the SFI and FBUS models with the experimental response of the RC shear wall specimen.

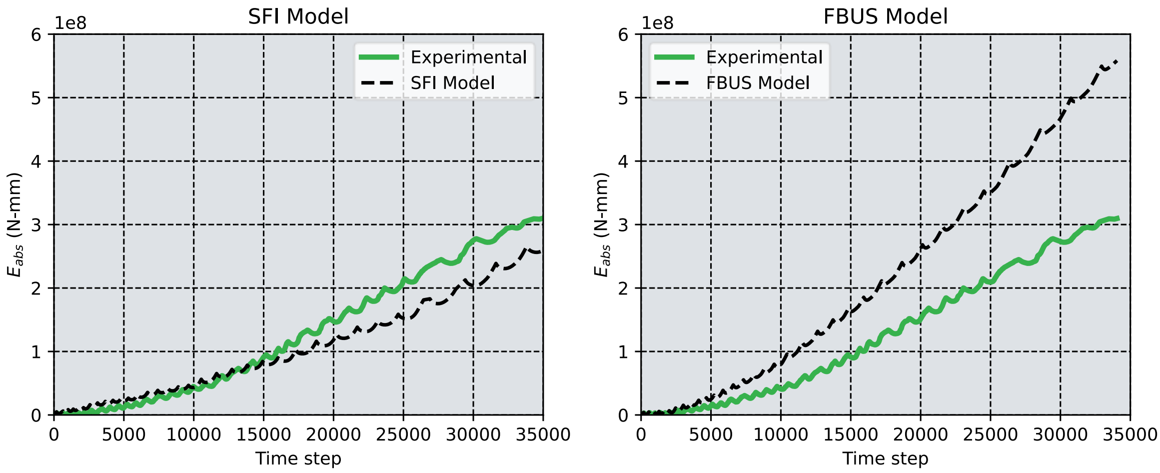

Figure 4. Comparison of the absorbed energy (E_{abs}) time history predicted by the SFI and FBUS models with the one obtained from the experimental response of the RC shear wall specimen.

As it is shown in Figure 3, the SFI model is capable of predicting the experimental hysteretic response of the RC shear wall accurately. As it was mentioned in Section 2, this modelling approach accounts for the interaction between the axial-flexural and shear responses of the RC shear wall. Furthermore, this model employs 2D RC panel behaviour that incorporates biaxial softening effects, including compression softening and hysteretic biaxial damage. Shear aggregate interlock effects in concrete, and dowel action for steel reinforcement are also accounted for using simplified constitutive relationships. These features allow the SFI models to simulate more accurately the base shear levels, and more notably, the unloading stiffness variation with displacement than the FBUS model. As a result, the absorbed energy time history (Figure 4) predicted by the SFI model closely matches the one obtained experimentally, since the predicted level of base shear and the unloading stiffness directly affect the level of energy dissipated by the RC shear wall specimen. On the other hand, the FBUS model tends to slightly overestimate the base shear experienced by the RC shear wall when compared to the experimental hysteretic response (Figure 3). Additionally, the unloading stiffness of the hysteretic response is greatly overestimated in the FBUS model. This produces that the absorbed energy is also overestimated significantly in the case of the FBUS model (Figure 4). One important aspect that must be highlighted is that one of the reasons that the SFI model performs better than the FBUS model for this RC shear wall specimen, is that the M/Vl ratio of this shear wall is approximately equal to 1.5; therefore, suggesting that shear deformations have a significant influence in the overall response of the shear wall. For RC shear walls exhibiting higher M/Vl ratios, an improved performance of FBUS models is expected [6,9].

To compare the potential accuracy and computational efficiency of the SFI and FBUS models to quantify SFMFs, fragility curves were derived using the two modelling approaches through IDA. To conduct the IDA, a set of 22 ground motion records including 11 records from shallow crustal sources, and 11 records from inslab sources was selected and scaled based on Method A specified in the NBC. All of the ground motion records were selected from the NGA West database [18]. The uniform hazard spectrum (UHS) with a probability of exceedance equal to 2% in 50 years specified by the NBC for a Site Class D in Vancouver, British Columbia was used as the target spectrum. Figure 5 shows the obtained mean 5%-damped ground response spectrum and the corresponding record-to-record variability envelope of the selected shallow crustal and inslab earthquakes. More information on the ground motion selection and scaling can be found in Dolati et al. [19].

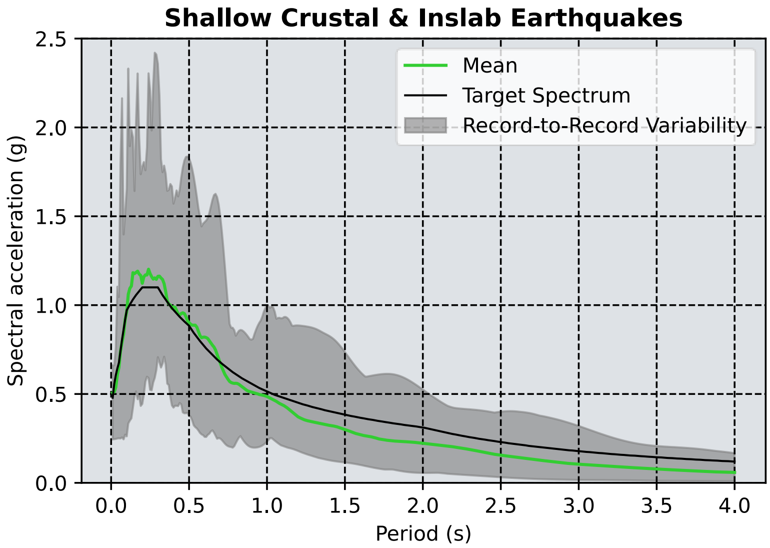

Figure 5. Mean ground response spectrum and record-to-record variability envelope of the selected shallow crustal and inslab earthquakes.

To derive fragility curves through IDA, a target limit state must be defined in order to evaluate the intensity measure value at which its exceedance takes place (IM_i). For this illustrative comparison, the ultimate deformation (Δ_u) of the shear wall was selected as the target limit state. To obtain the ultimate deformation of the shear wall, the approach specified in FEMA P-795 [20] was considered. Additionally, the ultimate load (Q_M) and initial stiffness (K_I) of the shear wall specimen were also obtained following the FEMA P-795 procedure. Figure 6 illustrates the approach specified by FEMA P-795 to calculate the Q_M, K_I, and the Δ_u parameters based on the envelope of the hysteretic response of the shear wall specimen. The Q_M parameter is taken as the maximum base shear value, the K_I parameter is taken as the stiffness based on base shear and displacement at $0.4Q_M$, and the Δ_u parameter is taken as the displacement at $0.8Q_M$. The derivation of the fragility curve was conducted following the approach specified by Baker [21] using a lognormal cumulative distribution function. The spectral acceleration at the vibration period of the shear wall specimen [$S_a(T_1)$] was considered as the intensity measure (IM) for the derivation of the fragility curves.

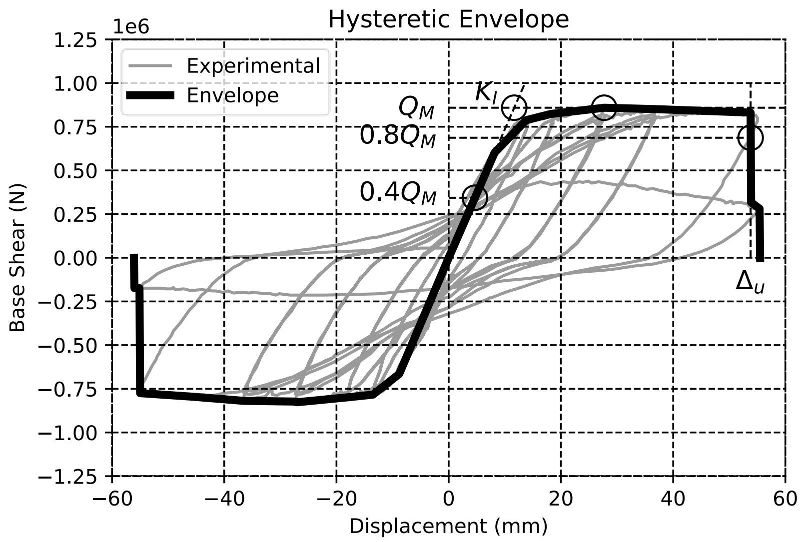

Figure 6. Determination of the Q_M, K_I, and Δ_u parameters according to FEMA P795 [20].

With regards to the execution of the IDA, the mass applied to the wall specimen in the NLTHAs was determined iteratively by evaluating the maximum displacement at the top of the shear wall for all of the selected ground motion records until the average of the maximum displacement was lower than the displacement corresponding to Q_M in the envelope curve. Since this illustrative comparison considers only the response of a single shear wall specimen, no additional sources of energy dissipation besides the hysteretic response of the wall were considered. Accordingly, no additional viscous damping was added to the numerical model.

The obtained IDA curves, and the derived lognormal fragility curves for the SFI and FBUS models are shown in Figure 7 and Figure 8, respectively. The values of the lognormal distribution parameters obtained from the fitting process are shown in Table 1, which are the median of the fragility curve (θ) and the dispersion (β).

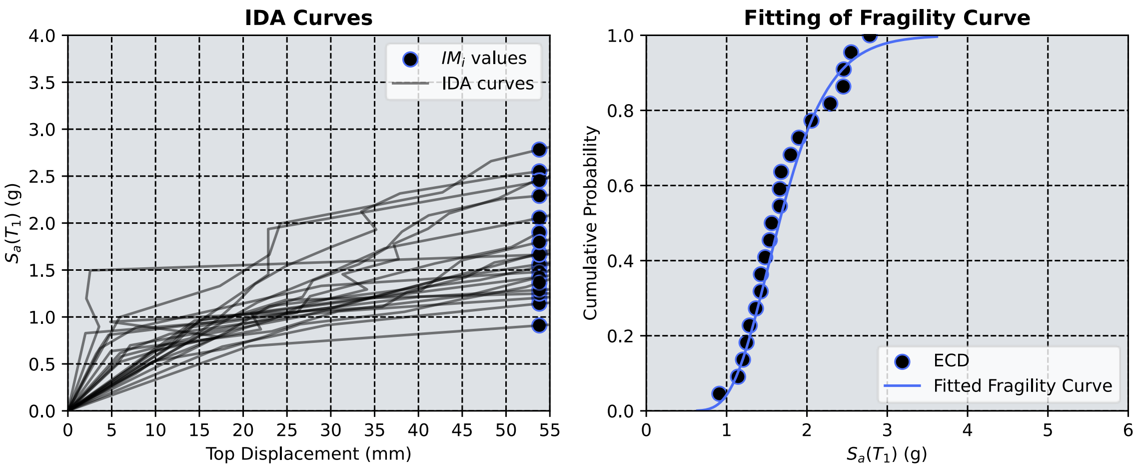

Figure 7. IDA curves and lognormal fragility curve fitted to the empirical cumulative distribution (ECD) obtained using the SFI model.

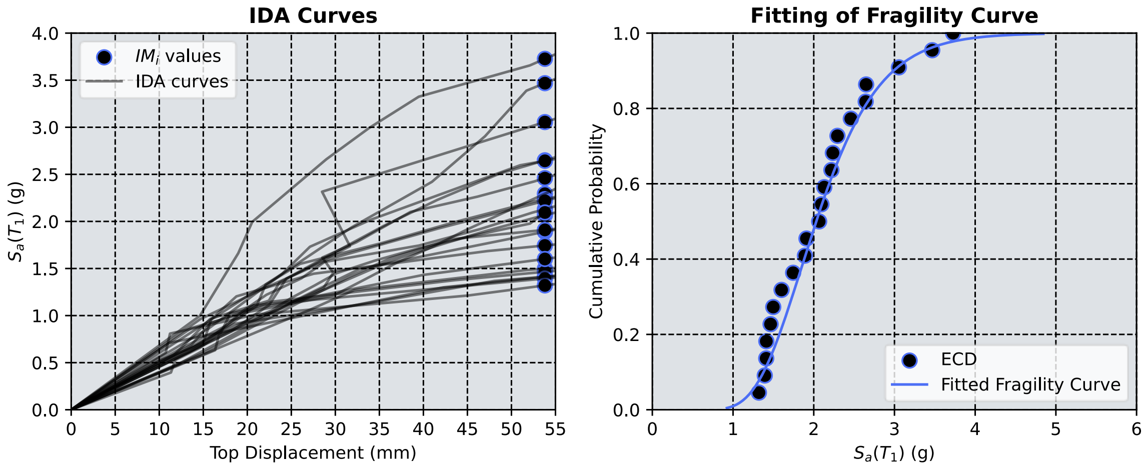

Figure 8. IDA curves and lognormal fragility curve fitted to the empirical cumulative distribution (ECD) obtained using the FBUS model.

Table 1. Parameter values of the fitted lognormal fragility curves.

	SFI model	FBUS model
$\theta\ (g)$	1.65	2.03
β	0.29	0.30

As it is shown in Figure 7 and Figure 8, implementing the FBUS model results in a higher median than when using the SFI model. The reason for the shift to the right of the fragility curve in the case of the FBUS model, can be explained by the slight overestimation of the base shear that this numerical model produces, since higher forces are required to achieve the same level of deformation than in the case of the SFI model. Additionally, as it is shown in Figure 4, the FBUS model significantly overestimates the absorbed energy of the shear wall specimen. This produces that for a given displacement level, the equivalent viscous damping ratio (ξ_{eq}) of the shear wall modelled with the FBUS approach will be significantly larger than in the case of the SFI approach. As a result, lower amplification of spectral accelerations is expected in the FBUS model. This can be validated by calculating the equivalent viscous damping ratio (ξ_{eq}) for both numerical models at a displacement equal to the ultimate deformation ($\Delta_u = 53.8\ mm$) using the Jacobsen equation [22,23], defined as:

$$\xi_{eq} = \frac{E_D}{2\pi k_{eff} \Delta_u^2} \tag{2}$$

where:
E_D= Energy dissipated in one cycle of the hysteretic response with displacement Δ_u.
k_{eff}= Effective stiffness at the displacement Δ_u.

Implementing Equation (2) results in an equivalent viscous damping ratio (ξ_{eq}) equal to 17% for the SFI model, and equal to 32% for the FBUS model; therefore, demonstrating that the FBUS model is expected to exhibit less amplification of the spectral accelerations.

With respect to the obtained values of dispersion (β), both models yielded very similar values. In the case of the SFI model, a dispersion equal to 0.29 was obtained, while in the case of the FBUS model it was equal to 0.30.

The obtained fragility curves highlight the importance of prioritizing SFI models when significant contribution of the shear deformations is expected in the overall response mechanism of the shear wall. Implementing FBUS models in such cases could result in an unrealistic over-performance of the SFRS.

Finally, when it comes to the computational time, there is a significant difference between the efficiency of the SFI and FBUS models. The computational time required to conduct the IDA using the SFI model was equal to 7,800 seconds using a computer with an 11^{th} Generation Intel Core i7-11850H processor, with a maximum single-core frequency of 2.50 GHz, and 32.0 GB of RAM. In the case of the FBUS model, using the same computer, the required computational time was equal to 540 seconds; therefore, showing a reduction of nearly 93% with respect to the SFI model. As it was briefly discussed in Section 2, the higher accuracy of the SFI model compared to the FBUS comes at the cost of significantly greater computational overhead. This is the main reason why, in the proposed procedure, the SFI model is recommended only for cases where a significant contribution of the shear deformations is expected in the overall response of a building archetype. Implementing this model for all of the building archetypes (which will exhibit a significantly larger number of degrees-of-freedom that the numerical models evaluated in this paper) and NLTHAs typically required to quantify SFMFs could make the process unfeasible due to the associated computational time and potential convergence issues.

4 CONCLUSIONS

To quantify seismic force modification factors (SFMFs) for their inclusion in the National Building Code of Canada (NBC), it is crucial to characterize the behavior of the target seismic force-resisting system (SFRS). This involves selecting modelling approaches for various building archetypes that accurately simulate seismic response while maintaining computational efficiency, as a significant number of non-linear time history analyses (NLTHAs) are often required. For the case of reinforced concrete (RC) shear wall buildings, the National Research Council Canada is conducting efforts to quantify their corresponding SFMFs specified in the NBC. This paper summarizes a systematic procedure to select the numerical modelling approach of RC shear wall building archetypes designed according to the NBC depending on their geometric, and behavioral characteristics to quantify their SFMFs.

The proposed procedure is based on two decision levels to determine the modelling approach that provides the best accuracy-efficiency tradeoff. The first decision level addresses whether the archetype exhibits torsional sensitivity or not to determine if 3D or planar numerical models should be considered. The second decision level considers the response mechanism that is expected to govern the overall seismic response of the archetype, in order to determine if the shear and axial-flexural interaction will play a significant role. Depending on the expected influence of shear deformations in the overall response, cyclic shear-flexure interaction models (SFI models) or fiber-based models with uncoupled shear springs (FBUS models) are recommended.

A simple comparison between the simulated response of a RC shear wall specimen using planar SFI and FBUS models is provided to illustrate the rationale behind the definition of the procedure. The accuracy of the numerical models is evaluated based on the hysteretic response of the RC shear wall, and the corresponding absorbed energy time history. To evaluate the potential impact of implementing the SFI and FBUS models to quantify SFMFs, fragility curves were derived using the two models through incremental dynamic analysis (IDA). The obtained results highlight the importance of considering SFI models in cases in which the shear deformations are expected to significantly contribute to the overall response mechanism of the RC shear walls. On the other hand, implementing the SFI modelling approach to all of the RC shear wall building archetypes is likely to be unfeasible, due to the associated computational burden and potential convergence issues. As a result, FBUS models are prioritized when axial-flexural deformations are expected to be dominant.

REFERENCES

[1] Housner GW. Historical View of Earthquake Engineering. Proceedings of the 8th World Conference on Earthquake Engineering, San Francisco, California: 1984.

[2] NRC. National Building Code of Canada: 2020 2022.

[3] FEMA. Quantification of Building Seismic Performance Factors, FEMA P695. Federal Emergency Management Agency (FEMA); 2009.

[4] Fazileh F, Fathi-Fazl R, Dolati A, Ventura CE, Saatcioglu M, Lau D, et al. Methodology for determination of seismic force modification factors in Canada: Performance-based unified procedure. Earthquake Spectra 2023;39:218–41. https://doi.org/10.1177/87552930221144325.

[5] CSA. Design of concrete structures, CSA-A23.3:24 2024.

[6] Orakcal K, Wallace JW. Flexural modeling of reinforced concrete walls - Experimental verification. ACI Structural Journal 2006;103:196–206.

[7] Kolozvari K, Orakcal K, Wallace JW. New opensees models for simulating nonlinear flexural and coupled shear-flexural behavior of RC walls and columns. Computers & Structures 2018;196:246–62. https://doi.org/10.1016/j.compstruc.2017.10.010.

[8] NIST. Evaluation of the FEMA P-695 Methodology for Quantification of Building Seismic Performance Factors. National Institute of Standards and Technology; 2010.

[9] Applied Technology Council. Modeling and Acceptance Criteria for Seismic Deisgn and Analysis of Tall Buildings. 2010.

[10] Galano L, Vignoli A. Seismic Behavior of Short Coupling Beams with Different Reinforcement Layouts. SJ 2000;97:876–85. https://doi.org/10.14359/9633.

[11] Naish D, Fry A, Klemencic R, Wallace J. Reinforced Concrete Coupling Beams—Part I: Testing. SJ 2013;110:1057–66. https://doi.org/10.14359/51686160.

[12] Tran TA, Wallace JW. Cyclic Testing of Moderate-Aspect-Ratio Reinforced Concrete Structural Walls. SJ 2015;112:653–65. https://doi.org/10.14359/51687907.

[13] McKenna F, Fenves G, Scott M. Open System for Earthquake Engineering Simulation 2000.

[14] Hunter JD. Matplotlib: A 2D Graphics Environment. Computing in Science & Engineering 2007;9:90–5.

[15] Kolozvari K, Orakcal K, Wallace JW. Modeling of Cyclic Shear-Flexure Interaction in Reinforced Concrete Structural Walls. I: Theory. Journal of Structural Engineering 2015;141:04014135. https://doi.org/10.1061/(ASCE)ST.1943-541X.0001059.

[16] Kolozvari K, Orakcal K, Wallace JW. SFI MVLEM - Cyclic Shear-Flexure Interaction Model for RC Walls 2016. https://opensees.berkeley.edu/wiki/index.php/SFI_MVLEM_-_Cyclic_Shear-Flexure_Interaction_Model_for_RC_Walls.

[17] Pugh JS. Numerical Simulation of Walls and Seismic Design Recommendations for Walled Buildings. University of Washington, 2012.

[18] University of California, Berkeley. PEER NGA-West Dataset 2008.

[19] Dolati A, Fazileh F, Fathi-Fazl R, Saatcioglu M, Huang X, Sayed MA. Seismic Performance Assessment of Conventional and Ductile Conrete Moment Frames Using Performance-Based Unified Procedure. Canadian Journal of Civil Engineering 2023.

[20] FEMA. Quantification of Building Seismic Performance Factors: Component Equivalency Methodology, FEMA P-795. Federal Emergency Management Agency (FEMA); 2011.
[21] Baker JW. Efficient Analytical Fragility Function Fitting Using Dynamic Structural Analysis. Earthquake Spectra 2015;31:579–99. https://doi.org/10.1193/021113EQS025M.
[22] Jacobsen L. Damping in composite structures. 2nd World Conference in Earthquake Engineering, Tokyo and Kyoto, Japan: 1960, p. 1029–44.
[23] Priestley M, Calvi GM, Kowalsky M. Displacement-Based Seismic Design of Structures. Pavia: IUSS Press, Istituto Universitario di Studi Superiori di Pavia; 2007.